



ELSEVIER

Journal of Chromatography A, 794 (1998) 129–146

JOURNAL OF  
CHROMATOGRAPHY A

# Investigation of photochemical behavior of pesticides in a photolysis reactor coupled on-line with a liquid chromatography–electrospray ionization tandem mass spectrometry system Application to trace and confirmatory analyses in food samples

Dietrich A. Volmer<sup>1</sup>

*Institute for Marine Biosciences, National Research Council, 1411 Oxford Street, Halifax, Nova Scotia B3H 3Z1, Canada*

## Abstract

The photochemical behavior of pesticides in a photolysis reactor coupled on-line with a liquid chromatography–electrospray ionization mass spectrometer (LC–hν-MS) was investigated. This paper describes the application of LC–hν-MS, in combination with tandem mass spectrometry (MS–MS), to identification of phototransformation products and to the establishment of possible photolytic pathways of pesticides. In addition, the applicability of LC–hν-MS as an alternative to LC–MS–MS, for trace and confirmatory multiresidue analysis in food samples was investigated. To demonstrate the potential of this technique, a series of N-heterocyclic compounds, phenylureas and carbamates, was studied. Several parameters, such as irradiation time and nature of photosensitizers, were investigated, and their impact on the photolytic transformation is presented here. The technique's versatility is also exhibited by using it for identification of triazine isomers, and for detection of pesticide residues in food sample extracts. Illustrative applications for analysis in lettuce and blueberry extracts are described. © 1998 Elsevier Science B.V.

**Keywords:** Liquid chromatography–mass spectrometry; Photolysis reactor; Pesticides

## 1. Introduction

Since many agricultural chemicals react in the environment under the influence of sunlight to form new, potentially harmful transformation products, photodegradation studies of pesticides have received much attention [1–4]. Most studies have been carried out in the laboratory under conditions designed to approximate those found in the field, that is, in aqueous solution in the presence of oxygen. Usually, the phototransformation products have been isolated

or separated by techniques such as thin-layer chromatography (TLC), gas chromatography (GC) or liquid chromatography (LC), often with fraction collection, and subsequently have been identified by mass spectrometry (MS) and/or nuclear magnetic resonance (NMR), ultraviolet (UV) and infrared (IR) spectroscopy. The phototransformation products are often present at trace levels which cannot always be separated and isolated. The procedures involved in general are time consuming, and an unambiguous identification of phototransformation products is often not readily possible because of fundamental limitations, e.g., thermal lability, co-eluting compounds, high polarities of photooxidation products, etc.

<sup>1</sup>Address for correspondence: Merck KGaA, Central Research Analysis (ZD-A/ZFA), Frankfurter Str. 250, D-64271 Darmstadt, Germany.

The on-line combination of liquid chromatography and mass spectrometry (LC–MS) offers significant analytical advantages over the aforementioned techniques. It allows the detection of polar and thermally labile pesticides even of compounds with no strong UV chromophores [5–10]. LC–MS techniques also provide the specificity necessary for confirmation of identity, especially when two analytes co-elute. Moreover, combination with tandem mass spectrometry (MS–MS) provides identification of unknown compounds. The latter was very important for the present study because one major goal was to detect phototransformation products formed from selected precursor pesticides and to identify their chemical structures. LC–MS has been successfully applied to identification of photodegradation products [11–14].

In the present study photolytic transformation has been induced by an on-line photolysis approach. Post-column photoreactors usually have been used for photoactivation of pesticides prior to electrochemical [15] or fluorescence detection [16–18]. In this study, however, the photoreactor was coupled to the analytical system prior to MS detection (LC– $h\nu$ -MS). Consequently, MS data on photolysis products are obtained very soon after formation, and without the need for laborious manual handling steps. The kinetics of these photolysis reactions are largely dependent on parameters such as irradiation wavelength, residence time in the reactor, solvent composition, presence of photosensitizers etc. Hence, these parameters were investigated to evaluate their impact on the LC– $h\nu$ -MS experiments.

However, in this study on-line photolysis was also used for a quite different reason; viz. to enhance structural information in LC–MS spectra. The most common LC–MS ionization techniques—thermospray (TSP), electrospray (ESI) and atmospheric pressure chemical ionization (APCI)—yield primarily molecular mass information. That is, little fragmentation is observed to confirm the structure of the analyte. In-source collision-induced dissociation (CID) has been utilized as a means of producing structurally significant ions [9,19,20]. In-source CID, however, is often unreliable and can suffer from a significant loss in sensitivity. Furthermore, tandem mass spectrometers are not universally available. As an alternative approach, on-line photolysis can be

used to induce photolytic dissociations. After post-column irradiation and LC–MS ionization, the phototransformation products appear as apparent “product ions” in the mass spectrum, since the unreacted precursor compound and the photoreaction products all co-elute. The usefulness of LC– $h\nu$ -MS has been demonstrated for the detection and confirmation of N-nitrosodialkylamines in beer samples [21], for the characterization of nitrosation products in cosmetic raw materials [22], and for various compounds of forensic interest [23].

This paper has two main objectives: (1) to examine the photochemical behavior of several pesticides in a post-column photoreactor coupled on-line with an ESI LC–MS–MS system, to identify phototransformation products, and to establish possible photolytic pathways; and (2) to show the applicability of on-line LC– $h\nu$ -MS as an alternative approach to LC–MS–MS for both trace analysis and confirmatory analysis of pesticides in food samples by means of inducing photolytic dissociations. A series of N-heterocyclic compounds, phenylureas and carbamates was chosen for this study.

## 2. Experimental

### 2.1. Chemicals

All pesticides (purity >98%) were obtained from ChemService (West Chester, PA, USA) and were used without further purification. Acetone, dichloromethane, methanol (J.T. Baker, Phillipsburg, NJ, USA) and Milli-Q organic free water (Millipore, Bedford, MA, USA) were used as solvents. Acetophenone, benzophenone, sodium sulfate and formic acid were purchased from Fluka (Ronkonkoma, NY, USA).

### 2.2. Sample preparation

The food samples were extracted according to the standard Luke II method [8,24,25]. Briefly, the samples were first homogenized with acetone–water in a blender and subsequently filtered. The resulting extracts were cleaned up by passing them through C<sub>18</sub> Sep-Pak cartridges (Waters, Milford, MA, USA). Thereafter, liquid–liquid extraction was conducted

with dichloromethane. The dried organic phases were then evaporated and the volumes adjusted with acetone. Post-partition cleanups were performed with Accell Plus QMA and amino propyl (NH<sub>2</sub>) cartridges (Waters). After concentration of the extracts to near dryness under nitrogen, the resulting residues were dissolved in water–methanol (4:1, v/v).

### 2.3. Liquid chromatography

High-performance liquid chromatographic (HPLC) separation conditions used for the investigated pesticides are discussed in more detail elsewhere [8]. Briefly, HPLC work was performed using a 150×3.2 mm (5 μm particles) Ultracarb ODS 30 column (Phenomenex, Torrance, CA, USA) operated at a flow-rate of 0.6 ml/min. The mobile phase flow was delivered by a Constametric 4110 HPLC gradient pump (Thermo Separation Products, Riviera, FL, USA). The mobile phase consisted of a methanol–water gradient (20–95% methanol over 45 min). An additional post-column flow of 0.4% formic acid in methanol at 0.2 ml/min was applied (Fig. 1), using an LC-5000 syringe pump (Isco, Lincoln, NE, USA). The solvents used were carefully purged with helium. The samples were introduced using a Rheo-

dyne 7125 injector (Cotati, CA, USA) equipped with a 10-μl loop.

### 2.4. UV photolysis

A photochemical reactor (Aura Industries, Staten Island, NY, USA), fitted with PTFE knitted open tubular reactor coils (5, 10 and 15 m×0.25 mm I.D.) and an 8W, 254 or 366 nm ultraviolet bulb, was connected after the analytical column and the post-column mixing tee (Valco, Houston, TX, USA), followed by a 1:4.5 split prior to MS analysis (Fig. 1). Unless otherwise stated, a 10 m knitted reactor coil was used (a 10 m reactor coil results in an irradiation time of ca. 30 s at a flow of 1 ml/min). By changing the length of the knitted reactor coil and the mobile phase flow-rate, the residence time in the photolysis reactor was varied. Practical considerations, however, did not allow complete freedom of choice of irradiation times when LC–hν–MS was used in conjunction with HPLC because of flow-rate restrictions. Acetone and benzophenone were used as photosensitizers in several experiments, and they were added post-column to the mobile phase via the syringe pump and mixing tee (Fig. 1) at concentrations of 0.5% (v/v) and 1 mM, respectively.

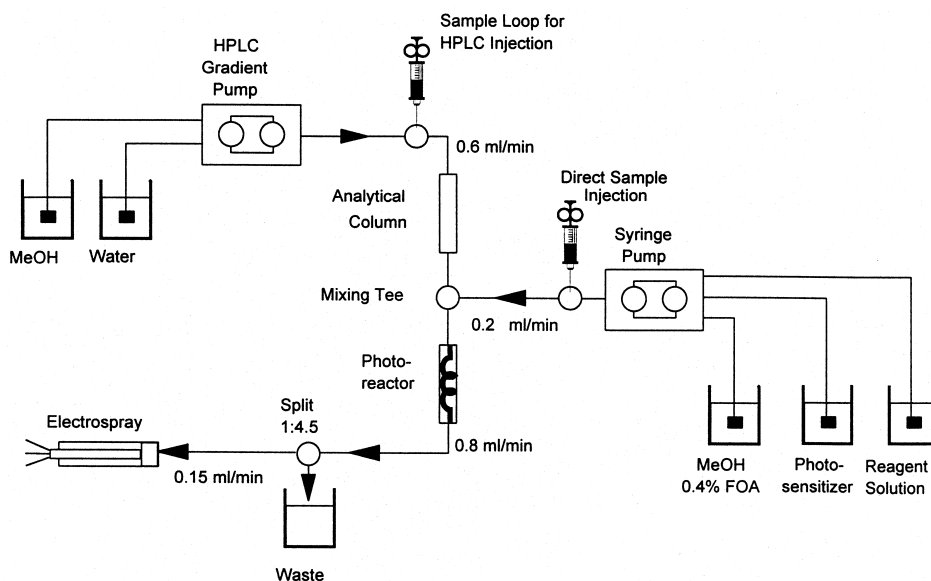


Fig. 1. Experimental setup.

### 2.5. Electrospray mass spectrometry

Approximately 150  $\mu\text{l}/\text{min}$  of eluent were admitted into the ESI source of a TSQ7000 triple-quadrupole mass spectrometer (Finnigan MAT, San José, CA, USA). Typical operating conditions for the MS were as follows: capillary temperature, 250°C; ESI voltage, 4.5 kV; sheath gas pressure,  $\approx 400$  kPa. For the identification of phototransformation products, the potentials in the transport region of the ESI source (heated capillary, tube lens and octapole collision-offset voltages) were reduced to lower than usual levels to prevent fragmentation of the more labile phototransformation products in the transport region of the ESI source. This was achieved by monitoring changes in the photolysis LC–MS spectra of all investigated pesticides upon lowering the lens potentials. Use of standard operating conditions of the interface led to in-source CID of phototransformation products in several cases, which made peak assignment in the photolysis LC–MS spectra more difficult or even impossible because mass spectrometric fragments of phototransformation products could falsely be assigned as intact quasi-molecular ions of products of photolysis reactions. CID was accomplished in the collision octapole using argon as collision gas at pressures between 1.0 and 1.6 mTorr (1 Torr=133.322 Pa) and collision-offset voltages between 15 and 35 V.

### 3. Results and discussion

The pesticide classes studied include triazines, other N-heterocyclic compounds, phenylureas and carbamates. The LC separation and ESI detection were carried out according to a recent multiresidue method for pesticides [8], and described briefly in Section 2.3.

The solvent type plays an important role in photolysis experiments as does pH, residence time in the photoreactor (irradiation time) and irradiation wavelength. Because the investigated target compounds did not show substantial absorption of UV light at irradiation wavelengths  $>300$  nm (and, consequently, no substantial phototransformations were observed in the LC–MS spectra), the following discussion describes the results obtained for an

irradiation wavelength of 254 nm. As mentioned above, in this study the reversed-phase solvent system methanol–water was used in experiments.

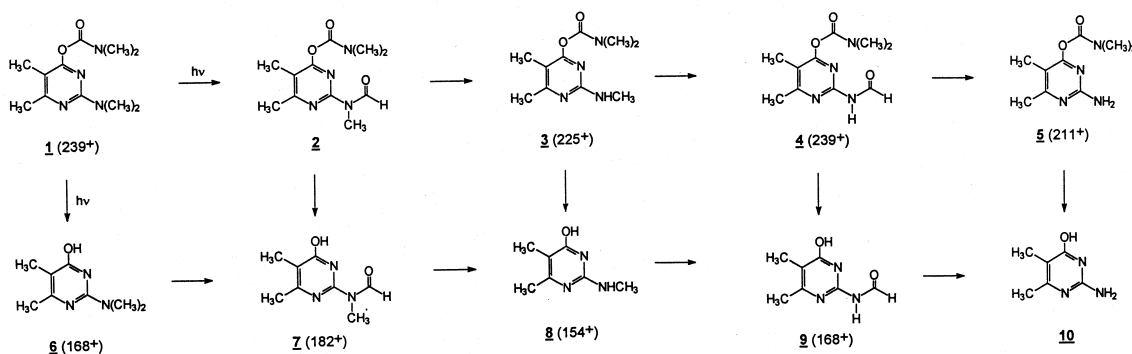
Photosensitizers such as acetone are often used to enhance the *o*-phthalaldehyde–2-mercaptoethanol (OPA–MERC) post-column fluorescence response for many pesticide classes [12]. Hence, their influence on the UV photolysis was studied. The chromophore of the photosensitizer typically absorbs photon energy and transfers it to the analytes, or the sensitizer itself forms a reactive species upon irradiation that can interact with the analytes. Acetone and benzophenone were chosen here because they have been shown [10–12] to enhance the OPA–MERC response of several of the compounds investigated in this study.

The results obtained using the on-line post-column photolysis LC–MS arrangement (Fig. 1) are discussed in the following text according to the chemical class of the target compounds.

#### 3.1. Phototransformation of pirimicarb and metamitron; influence of photosensitizers

The photodegradation of the N-dimethylcarbamate insecticide pirimicarb (2-[dimethylamino]-5,6-dimethylpyrimidin-4-yl-N-dimethylcarbamate **1**, refer to Scheme 1) has been extensively studied [26–34]. The compound has been shown to decompose rapidly on plants in the field. N-Formylpirimicarb (**2**) and N-desmethylpirimicarb (**3**) and several other oxygenated products, have been identified as toxic degradation products [26,27]. Photodegradation in the presence of organic solvents such as hexane, methanol and acetone, as representative model substances for the plant cuticle constituents, has been suggested by Schwack and Kopf [26] and Nag and Dureja [35].

UV photolysis of pirimicarb (**1**) at  $\lambda=254$  nm in methanol–water (pH 2.8) resulted in rapid degradation of the precursor compound (Fig. 2a and b). Within an irradiation time of 80 s, **1** was degraded by ca. 75%. The photolysis resulted in a number of products, the most abundant being N-desmethylpirimicarb (**3**) with  $\text{MH}^+$  at  $m/z$  225. This compound was probably formed by photooxidation via N-formylpirimicarb (**2**). The intermediate **2** could not be identified in the LC– $h\nu$ -MS spectrum but, as



Scheme 1. Non-sensitized photolysis LC–MS analysis of pirimicarb ( $\text{MH}^+$  at  $m/z$  239).

shown below, it was observed in the photosensitized reaction after stabilization with acetone.

Hydroxylation of the 5-methylpyrimidinyl moiety as suggested by Schwack and Kopf [26], could also be observed in our experiments. The ion at  $m/z$  255 indicates formation of 5-hydroxymethylpirimicarb. Structural MS–MS analyses (not shown) of additional degradation products with  $\text{MH}^+$  at  $m/z$  154, 168 and 182 were consistent with the proposed structures **6**, **7**, **8** and **9** (Scheme 1), and thus revealed a second series of photodegradation products starting with the hydrolysis of the carbamate function of pirimicarb (**1**). Photooxidation and decarbonylation of **6** then lead to 2-methylamino-5,6-dimethylpyrimidin-4-ol

(**8**) via **7** ( $m/z$  182). The predicted N-des-methylated product (2-amino-5,6-dimethylpyrimidin-4-ol, **10**) could not be observed in the products. In addition to these described photodegradation products, a number of other products were detected at trace levels (Fig. 2b).

On irradiation of pirimicarb in the presence of acetone as photosensitizer, but under otherwise identical experimental conditions, a wide variety of ions different from those obtained in the non-sensitized photolysis was obtained (Fig. 2c). This observation seemed to indicate completely different photolysis mechanisms for the photosensitized experiment. However, nearly all of these products

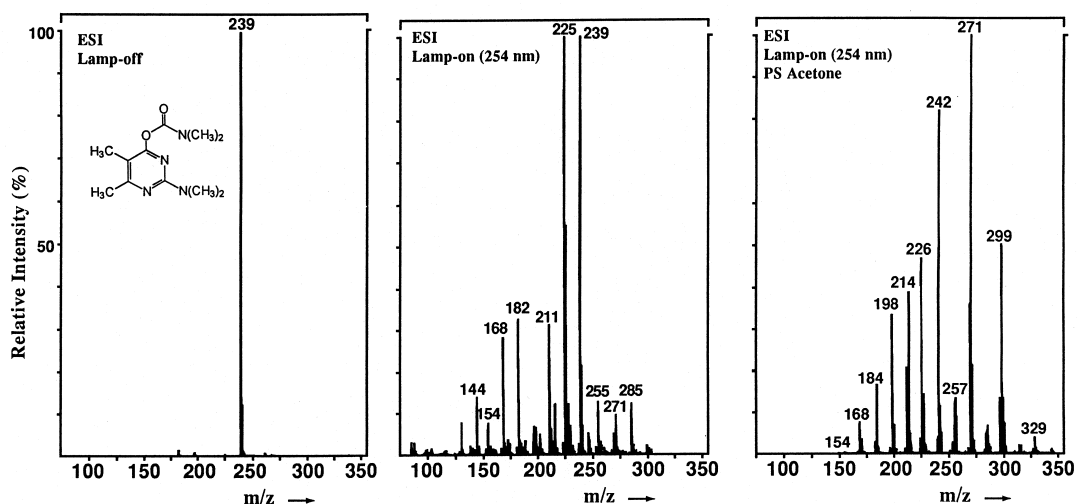
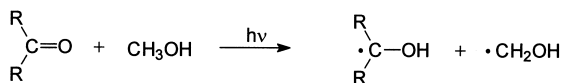


Fig. 2. LC–hv–MS analysis of pirimicarb ( $\text{MH}^+$  at  $m/z$  239). (a) Lamp-off, (b) lamp-on (no photosensitizer), (c) lamp-on, acetone-sensitized photolysis ( $\lambda=254$  nm, 10 m photoreactor).

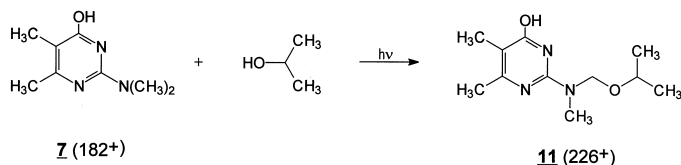


Scheme 2. Primary photolysis reaction in the solvent system methanol–water–acetone at  $\lambda=254$  nm.

could be identified and eventually related to the products given in Scheme 1. Most of the photolysis products in these and other experiments can be explained by considering the photolysis behavior of the sensitizers acetone and benzophenone.

The primary photodegradation reaction in the system methanol–water–acetone (or benzophenone) [36] at  $\lambda=254$  nm corresponds to photochemical reduction of acetone (benzophenone) carbonyl with hydrogen abstraction from methanol, resulting in  $\cdot\text{CH}_2\text{OH}$  and  $\cdot\text{C}(\text{CH}_3)_2\text{OH}$  radicals (Scheme 2). That is, adducts of the analytes and their transformation products with these radicals can be expected. These radicals can attack the nitrogen-activated 5,6-double bond of the pyrimidine moiety of pirimicarb and its degradation products with subsequent hydrogen atom ( $\cdot\text{H}$ ) transfer from the solvent to give  $[\text{MH}+32]^+$  and  $[\text{MH}+60]^+$  ions in the subsequent ESI-MS analysis.

As mentioned above, on-line tandem MS–MS analysis was performed on all photolysis product ions to confirm or elucidate the chemical structures of the phototransformation products (data not shown). Table 1 lists the ion/structure correlations between the sensitized and non-sensitized photolyses. Detection of photodegradation products with an intact carbamate function attached to the pyrimidine ring was straightforward. They all give rise to an abundant ion at  $m/z$  72 in the MS–MS spectrum corresponding to  $[(\text{CH}_3)_2\text{N}=\text{C}=\text{O}+\text{H}]^+$  (MS–MS data available from the author upon request). This ion could readily be used for precursor ion scanning to detect possible phototransformation products.



Scheme 3. Formation of the precursor compound for the ion at  $m/z$  226 in the acetone-sensitized photolysis of pirimicarb at  $\lambda=254$  nm.

Table 1

Structure assignment to  $m/z$  values in the acetone-sensitized LC– $h\nu$ –MS analysis of pirimicarb (refer to Scheme 1)

$m/z$	Assignment $[\text{+H}]^+$
313	<b>2</b> + $\cdot\text{C}(\text{CH}_3)_2\text{OH} + \cdot\text{H}$
299	<b>1</b> + $\cdot\text{C}(\text{CH}_3)_2\text{OH} + \cdot\text{H}$
285	<b>3</b> + $\cdot\text{C}(\text{CH}_3)_2\text{OH} + \cdot\text{H}$
271	<b>1</b> + $\cdot\text{CH}_2\text{OH} + \cdot\text{H}$
257	<b>3</b> + $\cdot\text{CH}_2\text{OH} + \cdot\text{H}$
242	<b>7</b> + $\cdot\text{C}(\text{CH}_3)_2\text{OH} + \cdot\text{H}$
228	<b>6</b> + $\cdot\text{C}(\text{CH}_3)_2\text{OH} + \cdot\text{H}$
226	<b>7</b> + $\cdot\text{C}(\text{CH}_3)_2\text{OH} - \cdot\text{H}$
214	<b>8</b> + $\cdot\text{C}(\text{CH}_3)_2\text{OH} + \cdot\text{H}$
212	<b>8</b> + $\cdot\text{C}(\text{CH}_3)_2\text{OH} - \cdot\text{H}$
200	<b>6</b> + $\cdot\text{CH}_2\text{OH} + \cdot\text{H}$
198	<b>7</b> + $\text{O}(-\text{CH}_3 \rightarrow -\text{CH}_2-\text{OH})$
184	<b>6</b> + $\text{O}(-\text{CH}_3 \rightarrow -\text{CH}_2-\text{OH})$

There are a few exceptions to the general rule that photosensitized reaction products correspond to simple photosensitizer adducts of non-sensitized photolysis products. An interesting example is the ion at  $m/z$  226, which has no corresponding precursor in Scheme 1. MS–MS analysis of that product suggested the structure **11** (Scheme 3), an adduct of isopropanol to the methyl group in the 2-dimethylamino side chain. A similar product has been observed by Schwack and Kopf [26] by irradiation of pirimicarb at  $\lambda=280$  nm in isopropanol. The ions at  $m/z$  184 and 198 (Table 1) in the acetone-sensitized LC– $h\nu$ –MS spectrum correspond to hydroxylation of the 6-methylpyrimidinyl moiety of **6** and **7** (these products were also present in trace levels in the non-sensitized photolysis, see Fig. 2b).

The photolysis in the presence of benzophenone instead of acetone was consistent with the results described for acetone. The adduct ions resulting from addition of  $\cdot\text{CH}_2\text{OH}$  radicals were still observed along with very intense ions corresponding to  $\cdot\text{C}(\text{Phe})_2\text{OH} (+\cdot\text{H})$  radical adduct ions, resulting in  $[\text{MH}+184]^+$  signals. In particular,  $m/z$  437 ( $=[\text{2} + 184 + \text{H}]^+$ , 10% relative abundance), 423 ( $=[\text{1} +$

$184+H]^+$ , 25%),  $409 (= [3+184+H]^+$ , 10%),  $395 (= [5+184+H]^+)$  and  $366 (= [7+184+H]^+$ , 55%) were identified and characterized. As for the acetone experiment, the methanol adduct ( $m/z$  271) was the main product in the benzophenone-sensitized photolysis.

Very similar types of adducts were observed in the acetone-sensitized photolysis of metatritron (A), a triazinone herbicide. The regular ESI spectrum under lamp-off conditions exhibited predominantly the usual  $MH^+$  ion (Fig. 3a). When the UV lamp ( $\lambda = 254$  nm) was turned on, but no acetone was added post-column to the LC-hv-MS system, the base peak was at  $m/z$  188, which corresponds to the photochemical reduction product desaminometatritron (B) (Fig. 3b). Desaminometatritron has been reported previously as the major photochemical degradation product of metatritron [37–39]. In the acetone-sensitized UV photolysis, adduct ions of these species with  $\cdot CH_2OH (+\cdot H)$  and  $\cdot C(CH_3)_2OH (+\cdot H)$  and a second photochemical reduction product of metatritron at  $m/z$  207, among numerous other trace products at higher masses (Fig. 3c) were observed.

### 3.2. Analysis of *s*-triazines by on-line UV photolysis

The hydroxy metabolites of *s*-triazines have been

reported as significant photodegradation products in aqueous environmental systems [40,41]. Photolysis of 2-chloro-*s*-triazines in the presence of solvents such as methanol–water leads to a number of products including some where the chlorine has been replaced by a methoxyl group [1,3,14,18].

In this study, seven triazines were investigated by LC-hv-MS in methanol–water (50:50, v/v)+0.1% formic acid. Dehalogenation was found to be the main degradation process for 2-chloro-*s*-triazines, to yield hydroxy- and methoxy-atrazine in methanol–water. With 2-methylthio-*s*-triazines substitution of the methylthio group by hydrogen or hydroxyl was the dominant process but no methoxylated products were obtained. To a smaller extent, dealkylation in the side chains was observed (these dealkylation reactions are discussed in more detail in Section 3.3). The results of our studies are summarized in Table 2. The degradation yields were high in all experiments. Fig. 4 shows the relative degradation yields for propazine and prometryn at various irradiation times.

The structures of all degradation products were confirmed by MS–MS (data available from the author upon request). To illustrate the structural elucidation of these products, Scheme 4 shows the MS–MS fragmentation pathway for the precursor compound atrazine and one of its degradation products.

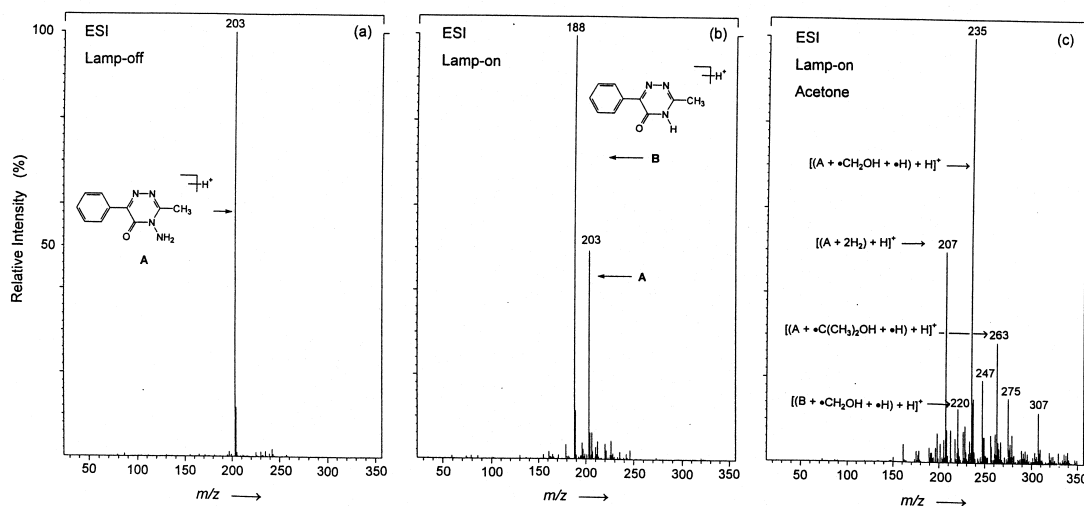


Fig. 3. LC-hv-MS analysis of metatritron (metatritron A,  $MH^+$  at  $m/z$  203; desaminometatritron B,  $MH^+$  at  $m/z$  188). (a) Lamp-off, (b) lamp-on (no photosensitizer), (c) lamp-on, acetone-sensitized photolysis ( $\lambda = 254$  nm, 10 m photoreactor).

Table 2  
LC-hv-MS analysis of 2-chloro and 2-methylthio-*s*-triazines<sup>1</sup>

Compound	R <sup>1</sup> , R <sup>2</sup>	Lamp-off MH <sup>+</sup> ( <i>m/z</i> )	Lamp-on			<i>I</i> <sub>m</sub> <sup>*</sup> / <i>I</i> <sub>m</sub>
			a	b	c	
X = Cl						
Atrazine	R <sup>1</sup> = C <sub>2</sub> H <sub>5</sub> R <sup>2</sup> = C <sub>3</sub> H <sub>7</sub>	216	198	212	–	1.0
Atrazine-desisopropyl	R <sup>1</sup> = C <sub>2</sub> H <sub>5</sub> R <sup>2</sup> = H	174	156	170	–	0.95
Simazine	R <sup>1</sup> = C <sub>2</sub> H <sub>5</sub> R <sup>2</sup> = C <sub>2</sub> H <sub>5</sub>	202	184	198	–	1.0
Propazine	R <sup>1</sup> = C <sub>3</sub> H <sub>7</sub> R <sup>2</sup> = C <sub>3</sub> H <sub>7</sub>	230	212	226	–	1.0
Terbutylazine	R <sup>1</sup> = C <sub>2</sub> H <sub>5</sub> R <sup>2</sup> = C <sub>4</sub> H <sub>9</sub>	230	212	226	–	1.0
X = SCH <sub>3</sub>						
Prometryn	R <sup>1</sup> = C <sub>3</sub> H <sub>7</sub> R <sup>2</sup> = C <sub>3</sub> H <sub>7</sub>	242	212	–	196	1.0
Terbutryn	R <sup>1</sup> = C <sub>2</sub> H <sub>5</sub> R <sup>2</sup> = C <sub>4</sub> H <sub>9</sub>	242	212	–	196	1.0

<sup>1</sup>Experimental conditions: methanol–water (50:50, v/v)+0.1% formic acid; 10 m reactor coil; flow-rate, 0.8 ml/min.

As shown in this study, the most important photochemical process for triazines was substitution of chlorine or methylthio groups by hydrogen, hydroxy or methoxy. Therefore, no substantial change in ionization efficiency of the products, as compared to the precursor compounds, should be expected. The change in ionization behavior is here expressed as  $I_m^*/I_m$  which is the ratio of the ion currents of the analytes with and without irradiation (lamp-on/lamp-off). That is, the integrated ion currents of all photodegradation product ions were divided by the ion currents of the precursor ions (MH<sup>+</sup> for the triazines). This quantity is essentially a measure of the relative ionization efficiency of the phototransformation products. In our experiments  $I_m^*/I_m$  values were approximately unity for all investigated triazines (Table 2).

The presence of photosensitizers did not seem to

alter the photochemical behavior substantially nor did changes in solvent composition, i.e., only two primary photolysis products were observed (Table 2) in varying compositions of methanol and water (results not shown). However, additional photodegradation products were observed in the presence of either acetone or benzophenone, particularly side chain reactions (see below) and adduct formation. As discussed above, the primary photolysis reaction in the water–methanol–acetone system is the formation of  $\cdot\text{CH}_2\text{OH}$  and  $\cdot\text{C}(\text{CH}_3)_2\text{OH}$  radicals, which in turn can add to activated double bonds such as those in substituted triazine ring systems. For example, the  $[(\text{M}-\text{Cl}+\text{OH})+\text{H}]^+$  ions at *m/z* 212 in the non-sensitized photolysis of prometryn and terbutryn (Table 2) were not observed in the acetone- or benzophenone-sensitized analysis. However, additional ions at *m/z* 228, 256 and 380 were observed



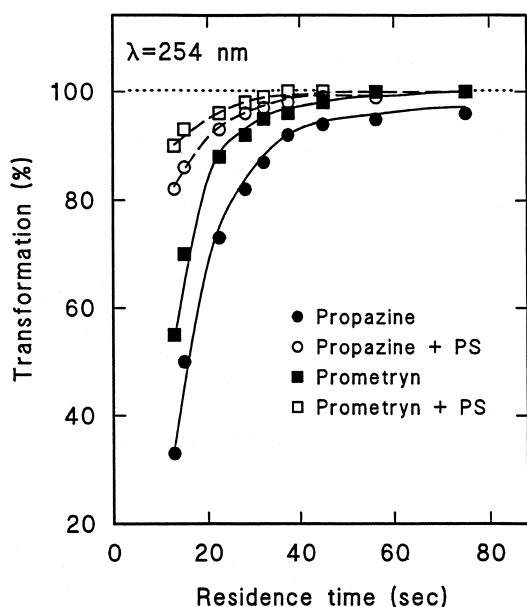


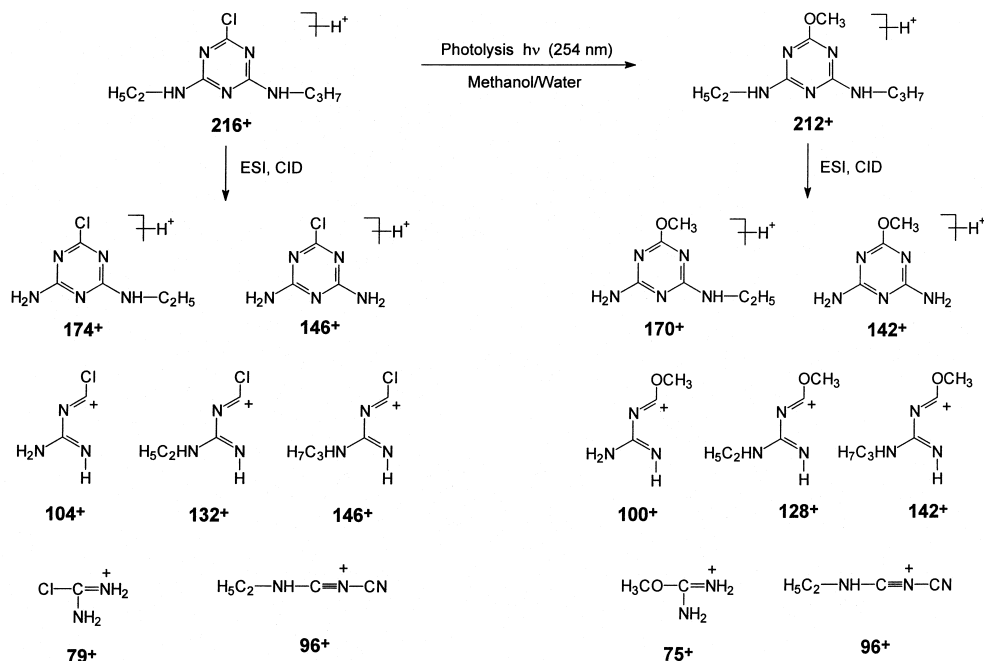
Fig. 4. Effect of irradiation time and photosensitizer (PS, acetone) on phototransformation of propazine and prometryn ( $\lambda=254$  nm).

with relative abundances up to 50%. These ions were probably formed by addition of  $\cdot\text{CH}_2\text{OH}$ ,  $\cdot\text{C}(\text{CH}_3)_2\text{OH}$  and  $\cdot\text{C}(\text{Phe})_2\text{OH}$  radicals (plus subsequent  $\cdot\text{H}$  transfer) to the triazine ring systems. In general, all triazines exhibited these methanol and acetone–benzophenone adducts to the ring system in the sensitized reaction. It should be noted again that these adduct ions are covalent adducts resulting from radical reactions. They are not adduct ions in the sense of simple van der Waals cluster adduct ions as are often observed in LC–MS spectra. This distinction can be most easily seen from the MS–MS analyses.

Practical applications of the photodegradation product ions illustrated above are described in Sections 3.3 and 3.4.

### 3.3. Characterization of triazine isomers by LC– $h\nu$ –MS

In this study two isomeric pairs of triazines have



Scheme 4. Identification of on-line photolysis products by LC–MS–MS. Proposed interpretation of main fragments of  $[\text{MH}]^+$  of atrazine ( $m/z$  216) and methoxyatrazine ( $m/z$  212).

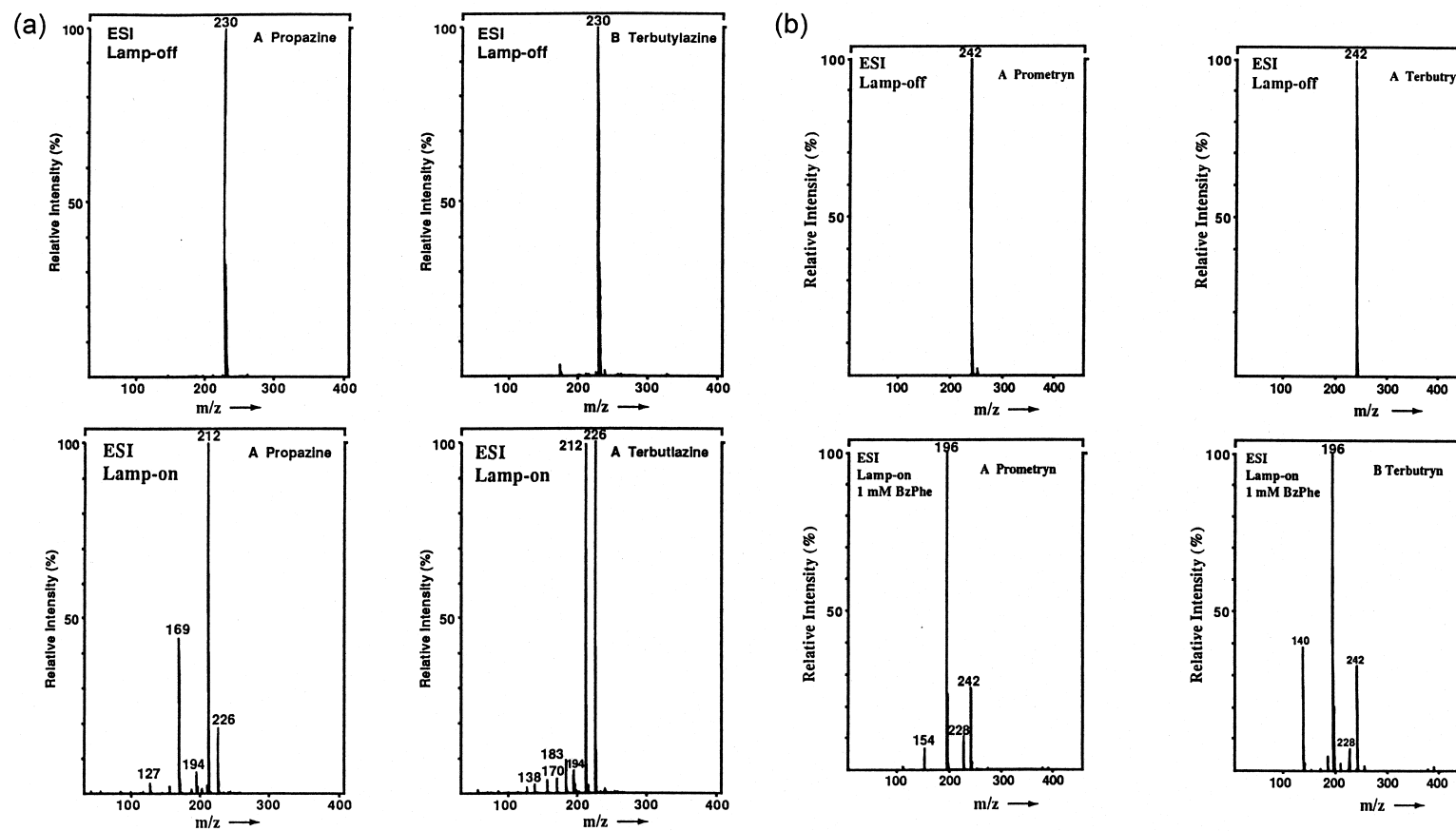
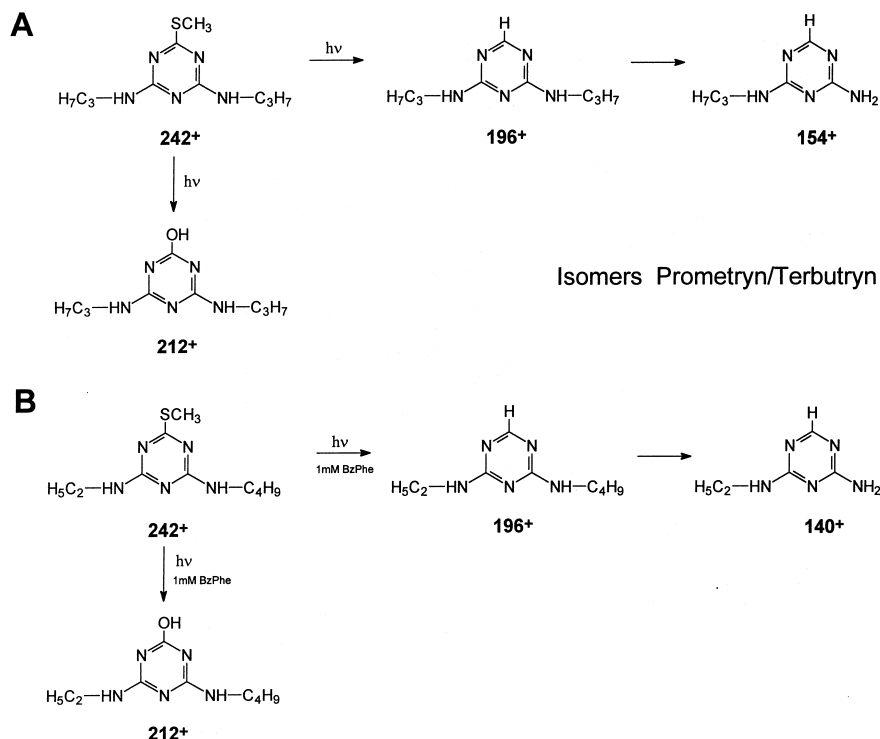


Fig. 5. LC-hv-MS characterization of the triazine isomer pairs propazine/terbutylazine and prometryn/terbutryn. (a) Propazine/terbutylazine; (b) prometryn/terbutryn.

been investigated, viz. propazine/terbutylazine and prometryn/terbutryn. Within each pair, these isomers differ only in the aminoalkyl substituents in the side chains (Table 2). One way to distinguish the individual isomers is, of course, MS–MS. In this study, however, a different approach was utilized. As mentioned in the previous section, photosensitization with acetone or benzophenone seemed to enhance dealkylation of the triazines. Therefore, if dealkylation occurs for only one of the aminoalkyl side chains of each isomer, isomer-specific ions should be formed by LC– $h\nu$ –MS. Fig. 5 summarizes the results of experiments which show that isomer-specific ions are formed at  $m/z$  169 and 183 for propazine and terbutylazine, respectively, and at  $m/z$  140 and 154 for prometryn and terbutryn (Scheme 5), respectively. The photolytic pathways for both pairs start with the replacement of the chloro or methylthio group by hydroxyl, methoxyl and/or hydrogen as discussed in Section 3.2. In this case, the methylthio group was preferentially replaced by hydrogen, and chlorine by hydroxyl and methoxyl groups. These substitution

products then underwent further degradation in the side chain to give isomer-specific ions. Surprisingly, the two pairs differ in their behavior concerning the side chain cleavage. Prometryn and terbutryn exhibited the expected dealkylation reaction (Scheme 5) whereas propazine and terbutylazine showed loss of the entire aminoalkyl side chain and replacement with hydrogen. The structures of these degradation products were confirmed by MS–MS (data not shown). Note that only for prometryn and terbutryn was a photosensitizer used in these experiments. Benzophenone greatly enhanced the dealkylation reaction for both compounds. For propazine and terbutylazine no such gain was observed which was most likely due to the different preferred initial substitution reactions, noted above.

Fig. 6 illustrates a practical example. It shows the identification of isomeric triazines in a spiked lettuce extract. A very short photoreactor (5 m length) was used in this experiment to ensure that both unreacted precursor ions ( $MH^+$ ) and photodegradation product ions were obtained. Four diagnostic ions were moni-



Scheme 5. Isomer-specific ion formation in the LC– $h\nu$ –MS analysis of prometryn (A) and terbutryn (B).

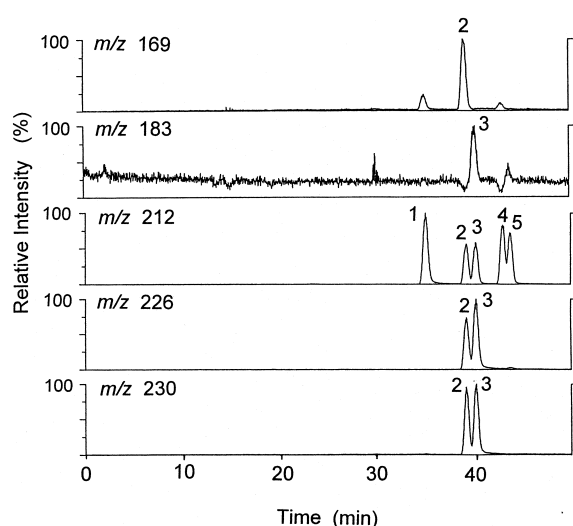


Fig. 6. Identification of isomers propazine and terbutylazine in a lettuce extract. LC-hv-MS chromatogram, (1) atrazine; (2) propazine (3) terbutylazine; (4) prometryn; (5) terbutryn (injected amount, ca. 5 ng each;  $\lambda=254$  nm, 5 m photoreactor).

tored for each of propazine and terbutylazine, including the isomer-specific ions at  $m/z$  169 and 183 discussed above. Without using the isomer-specific ions, identification of the individual isomers would only be possible based on retention times. In this case this would be difficult because the two isomers almost co-eluted. Furthermore, several other analytes gave interfering signals. Monitoring the isomer-specific photolysis ions at  $m/z$  169 and 183, however,

made peak assignment of both isomers readily possible (Fig. 6).

### 3.4. Evaluation of the LC-hv-MS method for determination of triazines in food samples

As described above, pesticide separation and determination were accomplished by means of a recently published multiresidue method for pesticides [8]. This method utilizes reversed-phase separation on a base-deactivated  $C_{18}$  column with a methanol-water gradient and post-column addition of formic acid. In this section, the adaptation of this method to LC-hv-MS is described. To evaluate the LC-hv-MS method for triazines, the linearity, limits of detection, precision and ruggedness were measured for the seven triazines investigated. External calibration curves were determined from the individual peak areas of the  $[(M-Cl+OH)+H]^+$  and  $[(M-Cl+OCH_3)+H]^+$  ions for the 2-chloro-*s*-triazines, and of the  $[(M-SCH_3+OH)+H]^+$  and  $[(M-SCH_3+H)+H]^+$  ions for the 2-methylthio-*s*-triazines, respectively. The results were compared with those from conventional ESI analyses under lamp-off conditions by using  $MH^+$  and  $[MH-R]^+$  ions (the  $[MH-R]^+$  fragment ions were generated in the transport region of the ESI source by in-source CID, see Table 3). The calibration curves were linear ( $r \geq 0.999$ ) from 20 pg to 100 ng injected on-column for both

Table 3

Comparison of conventional electrospray and photolysis electrospray (LC-hv-MS) for analysis of triazines

Compound	$t_r$ (min)	$M_n$	Quant. ions ( $m/z$ ) <sup>a</sup>	LOD (pg) <sup>b</sup>	LOD* (pg) <sup>b</sup>	R.S.D. (%) <sup>c</sup>	R.S.D.* (%) <sup>c</sup>	$f$ (25,50,80%) <sup>d</sup>
Atrazine-desisopropyl	12:55	173	174,156/156*,170*	5	10	4	9	0.82/0.90/0.92
Simazine	27:05	201	202,174/184*,198*	1	2	5	8	0.42/0.60/0.79
Atrazine	32:85	215	216,174/198*,212*	1	1	5	10	0.49/0.65/0.80
Propazine	36:85	229	230,188/212*,226*	0.5	1	4	10	0.85/0.98/1.51
Terbutylazine	37:98	229	230,174/212*,226*	0.5	1	3	6	0.96/1.34/1.88
Prometryn	40:55	241	242,200/196*,212*	0.2	0.5	3	9	0.31/0.36/0.51
Terbutryn	41:45	241	242,184/196*,212*	0.2	0.5	4	10	0.28/0.42/0.47

<sup>a</sup> Quantitation ions for time-scheduled SIM analysis (lamp-off/lamp-on, photolysis products are marked with an asterisk). Lamp-off, in-source CID offset voltage=20 V; lamp-on, in-source CID offset voltage=0 V.

<sup>b</sup> Limit of detection ( $S/N=3$ ); lamp-off, LOD; lamp-on, LOD\*.

<sup>c</sup> Precision of ion ratios between the two quantitation ions for replicate injections of 1 ng of each triazine ( $n=5$ ); lamp-off, R.S.D.; lamp-on, R.S.D.\*.

<sup>d</sup> Ion ratios are  $f=I[(M-Cl+OH)+H]^+/I[(M-Cl+OCH_3)+H]^+$  for chlorotriazines and  $f=I[(M-Cl+OH)+H]^+/I[(M-Cl+H)+H]^+$  for methylthiotriazines at 25, 50 and 80% (v/v) methanol.

methods, with very similar performance characteristics.

The SIM limits of detection (all data corresponding to the lamp-on mode of operation are marked with an asterisk, e.g., LOD\*) of the LC–hν–MS technique using the described two ions per compound, as estimated by a signal to noise ratio of 3:1 from the low end of the calibration curve, were 0.5–10 pg for the seven triazines which were very similar to those observed for the conventional analysis (LOD, 0.2–5 pg). The noise levels increased slightly in lamp-on mode as compared to the lamp-off conditions which, in turn, caused a slight increase of LOD\*. The LODs and LOD\*s were higher for early eluting compounds, and this general observation is probably related to the lower organic modifier content in the gradient mixtures at shorter retention times [8]. A very similar trend was observed for both LOD and LOD\*. Because the kinetics of the photolysis depends on the solvent composition and solvent pH, this may also have an effect on LOD\*.

In a regulatory environment, the ability of LC–hν–MS to provide stable and reproducible response over an extended period of time is of great importance. Hence, the precision was investigated by observing the short-term and long-term standard deviations of the relative abundances of ions of the photolysis products in comparison to conventional ESI (Table 3). It was observed that replicate injections gave slightly better relative standard deviations when using conventional ESI. Nevertheless, LC–hν–MS usually gave R.S.D.\*s for replicate injections of 10% or less. These slightly larger deviations may be attributed to changes in back pressure from the knitted photoreactor coils. The back pressure deviates over extended periods of time and subsequently changes the flow-rate (i.e., irradiation time) [21]. This effect can be clearly seen from the long-term precision values which were higher and usually ranged between 10 and 20% R.S.D.\* or sometimes even higher. Certain other compound classes such as phenylureas exhibited even larger deviations (see Section 3.5).

An important parameter in the investigation of the ruggedness of the LC–hν–MS method is the influence of the solvent composition on the LC–hν–MS spectra. As discussed earlier, the nature of the photolysis reactions is independent of the methanol–

water composition. The kinetics, however, are dependent on the solvent composition. To determine a possible influence of the solvent composition on the ion ratios,  $f = I[(M-Cl+OH)+H]^+ / I[(M-Cl+OCH_3)+H]^+$  or  $f = I[(M-SCH_3+OH)+H]^+ / I[(M-SCH_3+H)+H]^+$ , five replicate flow injections were made for each compound at three different solvent compositions of methanol–water: 25%, 50% and 80% (v/v). The results of these experiments are listed in Table 3, and show a marked dependence of  $f$  on the solvent composition. The values of precision obtained for  $f$  at a given solvent composition for replicate injections, however, were again  $\leq 10\%$  R.S.D..

Fig. 7 illustrates the application of LC–hν–MS to the analysis of a blueberry extract. The sample was spiked with four triazines (ca. 5 ng each) and two ions per compound were monitored (see Table 3). All compounds could readily be identified in the sample extract.

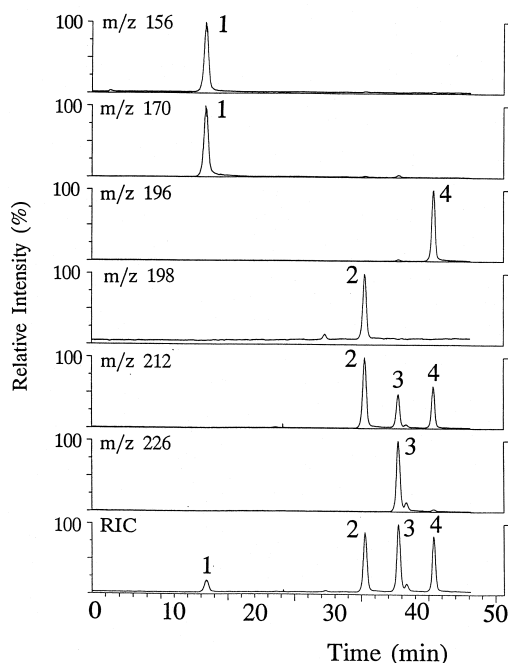


Fig. 7. LC–hν–MS chromatogram of a blueberry extract spiked with four triazines. (1) Atrazine-desisopropyl; (2) atrazine; (3) propazine; (4) terbutryn (injected amount, ca. 5 ng each;  $\lambda = 254$  nm, 5 m photoreactor).

### 3.5. Phototransformation of phenylureas

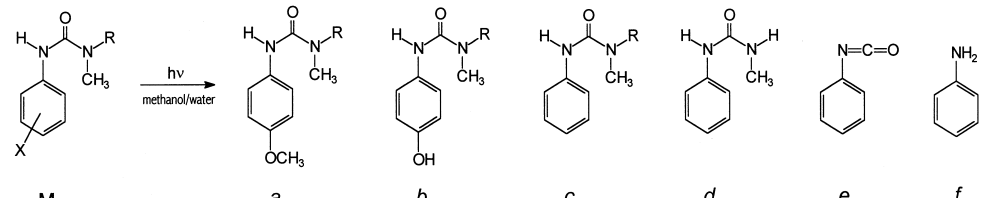
On-line UV photolysis of phenylureas in methanol–water resulted in a large number of transformation products (Table 4). The major degradation pathways of phenylureas are losses of halogen or phenoxy/alkoxy groups from the phenyl-ring and replacement by a hydroxyl or methoxyl group or hydrogen (structures a to f in Table 4), resulting in abundant  $[(M-X+H)+H]^+$ ,  $[(M-X+CH_3O)+H]^+$  and  $[(M-X+OH)+H]^+$  ions. The hydroxylated aromatic species give rise to enhanced fluorescence [17,18] in the fluorescence analysis after post-column photolysis. The di-halogenated phenylureas, diuron and linuron, exhibited almost complete substitution of both chlorine atoms. That is,  $[(M-2Cl+2H)+H]^+$ ,  $[(M-2Cl+CH_3OH)+H]^+$  and  $[(M-2Cl+H_2O)+H]^+$  ions were observed in the photolysis mass spectra. However, the low-abundance

signal at  $m/z$  199, with a corresponding  $^{37}\text{Cl}$  isotope signal ( $m/z$  201) in the spectrum from diuron probably corresponds to replacement of only one of the two chlorine atoms. The only unsubstituted compound investigated (fenuron) did not show strong UV photolysis, whereas photodegradation yields for most halogen-containing phenylureas investigated were close to 100%, even with a short photoreactor. In addition to the ions described above, numerous other phototransformation products were formed, especially in the  $m/z$  range above that of the  $\text{MH}^+$  ion. Formation of dimethylamine ( $m/z$  46), as reported by other authors [16,42,43], was also observed in the spectra of N,N-dimethylphenylureas in our experiments, with relative abundances up to 25%. Degradation to phenylisocyanate (structure e) and aniline (f) were also observed.

In the presence of acetone or benzophenone, the intense ions in the  $m/z$  range above that of the  $\text{MH}^+$

Table 4

Major phototransformation products and their relative abundances in the LC-hv-MS analysis of phenylureas<sup>1</sup>



Compound	R, X	Lamp-off	Lamp-on							
		$\text{MH}^+$	$\text{M}^*\text{H}^+$	a	b	c	d	e	f	Other ions
Chloroxuron	R = CH <sub>3</sub> X = OC <sub>6</sub> H <sub>4</sub> Cl	291(100)	291(5)	–	273(15) <sup>2</sup>	257(30) <sup>2</sup>	243(25) <sup>2</sup>	120(<1)	94(1)	319(50), 303(50), 289(40), 195(20), 147(20), 46(25)
Difenoxyuron	R = CH <sub>3</sub> X = OC <sub>6</sub> H <sub>4</sub> OCH <sub>3</sub>	287(100)	287(40)	–	–	165(60)	–	120(15)	94(5)	333(40), 319(40), 273(20), 79(100), 46(25)
Diuron	R = CH <sub>3</sub> X = 2Cl	233(100)	233(<1)	195(100)	181(30)	165(30)	–	120(10)	94(5)	259(15), 199(10), 243(20), 163(30), 150(25), 46(20)
Fenuron	R = CH <sub>3</sub> X = H	165(100)	165(100)	–	–	–	–	120(20)	94(5)	152(10), 46(5)
Linuron	R = OCH <sub>3</sub> X = 2Cl	249(100)	249(<1)	211(30)	–	181(95)	151(35)	–	94(10)	327(20), 297(20), 243(25), 196(25), 124(20)
Metobromuron	R = OCH <sub>3</sub> X = Br	259(100)	–	211(35)	197(30)	181(100)	151(55)	–	94(12)	327(20), 297(25), 243(25), 124(20), 79(90)

<sup>1</sup> Experimental conditions: 10 m photoreactor coil, irradiation at 254 nm; solvent, methanol–water (50:50)+0.1% formic acid at 1 ml/min.

<sup>2</sup> Substitution of the chlorine atom of the *p*-chlorophenoxy group.

ion, observed in the non-sensitized photolysis, mostly disappeared and photolysis almost exclusively yielded the above mentioned substitution products with very similar relative abundances to those observed in the non-sensitized reactions.

As shown by Mazzocchi and Rao [42], the major process in the photolysis in methanol of monuron, a mono-chlorinated N,N-dimethylphenylurea very similar to diuron and linuron, is cleavage of the C–Cl bond followed by hydrogen abstraction from the solvent to form the reduced product fenuron. Fenurons major photolysis pathway involved cleavage of the (carbonyl carbon)–nitrogen bond to give a radical pair with subsequent reaction to stable photo-products (e.g., aniline). These authors demonstrated [42] that monuron reacted about four times as fast as fenuron, that is, photolytic cleavage of the (carbonyl carbon)–nitrogen bond should not be an important process in the photolysis of halogenated/alkoxylated phenylureas. These findings are in agreement with the present results (Table 4). Fenuron did not show UV photolysis yields comparable to those obtained with ring-substituted phenylureas in our experiments. Photolysis resulted in the formation of the phenylisocyanate with  $MH^+$  at  $m/z$  120, and the reaction product of the isocyanate plus methanol at  $m/z$  152

### 3.6. Phototransformation of N-methylcarbamates

N-Methylcarbamates have been shown to produce significant amounts of methylamine upon photolysis [43–45]. Several authors (e.g., [16–18,46]) demonstrated the formation of primary amines from several pesticides including carbamates by using the OPA–MERC reagent for reaction with the amines to form strongly fluorescing compounds having an isoindole structure. The advantage of the present LC– $h\nu$ –MS system is that the extent of methylamine formation can easily be monitored as a function of the irradiation time. This might be helpful to find optimum conditions for methylamine formation for fluorescence detection. The six N-methylcarbamates listed in Table 5 were studied in the present work.

Fig. 8 illustrates the effect of irradiation time on several species formed from carbaryl.  $[MA]^+$  represents the integrated intensity of all quasi-molecular ions. As expected, the relative amount of methyl-

amine ( $[CH_3NH_3]^+$ ,  $m/z$  32) increased with increasing irradiation time. Methylamine adduct ions with the precursor compounds (to give  $[M+32]^+$ ) were also observed. Both  $[CH_3NH_3]^+$  and  $[M+CH_3NH_3]^+$  ions, however, completely disappeared when the lamp was turned off (Fig. 9). These  $[M+32]^+$  ions have also been observed with relative intensities up to 72% in the TSP–LC–MS analysis of oxime N-methylcarbamates by thermally-induced hydrolysis in the thermospray vaporizer and subsequent self-ionization of the precursor compounds by attachment of protonated methylamine in the gas-phase [47,48]. The proton affinity of methylamine is high (896 kJ/mol) so that it is readily ionized in the gas-phase. Acetone seemed to only slightly increase the formation of  $[CH_3NH_3]^+$  or  $[M+CH_3NH_3]^+$  (Table 5).

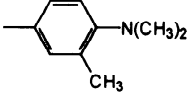
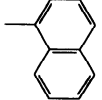
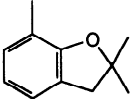
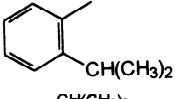
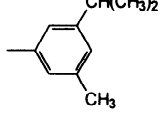
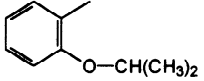
A possible application of these observations in LC–MS analyses would be the use of  $[M+32]^+$  ions for molecular mass confirmation, and of  $[CH_3NH_3]^+$  ions for class-specific screening of sample extracts for N-methylcarbamates. The specificity of such a screening procedure, however, would be low because other compound classes containing N,N-dimethyl groups have also been shown to produce methylamine [16–18] upon UV photolysis.

All investigated N-methylcarbamates exhibited the described photodegradation reactions except aminocarb, the photolysis mass spectrum of which was dominated by the ion at  $m/z$  136 (Table 5). This ion could possibly be assigned to a phototransformation product that results from replacement of the entire N-methylcarbamate chain at the phenyl ring by hydrogen. However, since aryl N-methylcarbamates are likely to undergo hydrolysis under the experimental conditions, and have also been shown to react in the *p*-dimethylamino side chain upon photolysis without other alteration in the molecules [17], cyclization (between *m*-methyl and *p*-dimethylamino) after hydrolysis to give an indoline ring structure also seems possible. No  $[CH_3NH_3]^+$  or  $[M+CH_3NH_3]^+$  ions were observed in the photolysis of aminocarb.

## 4. Conclusions

This study has demonstrated the applicability of

Table 5  
LC-h $\nu$ -MS analysis of N-methylcarbamates<sup>1</sup>

H <sub>3</sub> C-NH-C(O)-O-R	R=	Lamp-off	Lamp-on				Other relevant ions <sup>2</sup>
		MH <sup>+</sup>	M*H <sup>+</sup>	[M*+CH <sub>3</sub> NH <sub>3</sub> ] <sup>+</sup>	[CH <sub>3</sub> NH <sub>3</sub> ] <sup>+</sup>	[M*H <sup>+</sup> -CH <sub>3</sub> NCO] <sup>+</sup>	
Aminocarb		209(100)	209(15)	– <sup>3</sup>	32(3/5) <sup>3</sup>	152(10/10) <sup>3</sup>	136(100), 121(15), 46(15)
Carbaryl		202(100)	202(100)	233(90/100)	32(10/15)	145(55/65)	256(20)
Carbofuran		222(100)	222(100)	253(65/60)	32(10/15)	165(10/10)	–
Isoprocarb		194(100)	194(100)	225(35/30)	32(7/12)	137(10/12)	280(10), 258(25), 169(10)
Promecarb		208(100)	208(100)	239(20/20)	32(5/8)	151(15/10)	–
Propoxur		210(100)	210(100)	241(30/25)	32(20/25)	–	274(30), 261(15), 168(15)

<sup>1</sup> Experimental conditions: 10 m photoreactor coil, irradiation at 254 nm; solvent, methanol–water (50:50)+0.1% formic acid at 1 ml/min.

<sup>2</sup> Non-sensitized photolysis.

<sup>3</sup> The relative abundances of these ions are listed for both the non-sensitized and the acetone-sensitized UV photolysis (non-sensitized/acetone).

LC-h $\nu$ -MS to the identification of photodegradation products. This method allows researchers to analyze polar transformation products directly, making fraction collection or other time-consuming sample preparation steps unnecessary. Moreover, the utilization of LC-h $\nu$ -MS, especially in combination with MS-MS, offers distinct possibilities for fast structural elucidation of transformation products formed by photochemical reactions.

On-line photolysis can also be used to induce photolytic reactions to give structurally diagnostic product ions and thus in turn, to add a significant degree of selectivity to LC-MS analyses, as demon-

strated in this study for the trace level determination and confirmation of triazine herbicides in blueberry and lettuce extracts. Although the method does not approach the degree of selectivity provided by MS-MS methods, it can be an inexpensive alternative for many applications. Moreover, the structurally diagnostic ions it produces differ substantially from those obtained in MS-MS systems, but are nevertheless complementary to CID. This approach is certainly less expensive than MS-MS and could be particularly useful in single-quadrupole LC-MS systems where in-source CID is either not available (as in TSP) or does not give reliable or satisfactory results.



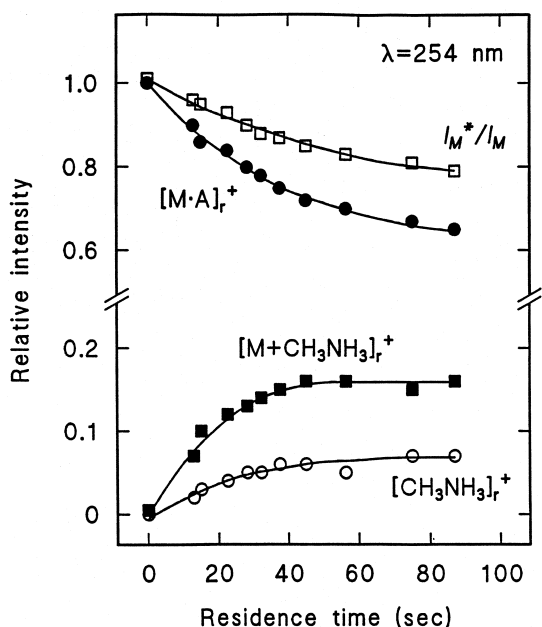


Fig. 8. Effect of irradiation time on  $[MA]^+$ ,  $[CH_3NH_3]^+$  and  $[M+CH_3NH_3]^+$  ion formation in LC-hv-MS of carbaryl ( $\lambda=254$  nm, no photosensitizer).

Chromatographic and other considerations required the solvent system methanol–water in this study. The type of photolysis and its kinetics are,

however, very often dependent on the solvent composition and pH as recently demonstrated for N-nitrosodialkylamines [21,22]. The investigation of different solvents and pH will be the focus of future research as will be the use of other photosensitizers with different sensitizing mechanisms, e.g., low energy triplet sensitizers such as Rose Bengal or chlorophyll to form singlet-oxygen. Further, photo-oxidation can transform analytes which do not give an adequate response in ESI or APCI into photo-products which do respond well.

### Acknowledgements

The author wishes to thank Dr. Jon G. Wilkes (USFDA, Jefferson, AR, USA) for many stimulating discussions, Dr. James A. Pincock (Dalhousie University, Halifax, Nova Scotia) for help with the interpretation of the photolysis mechanisms and Dr. Robert K. Boyd (Institute for Marine Biosciences, Halifax, Nova Scotia) for his valuable discussions and suggestions in the preparation of this manuscript. Part of this work has been carried out in laboratory facilities at the National Center for Toxicological Research (Jefferson, AR, USA) with financial support by the ORAU research program.

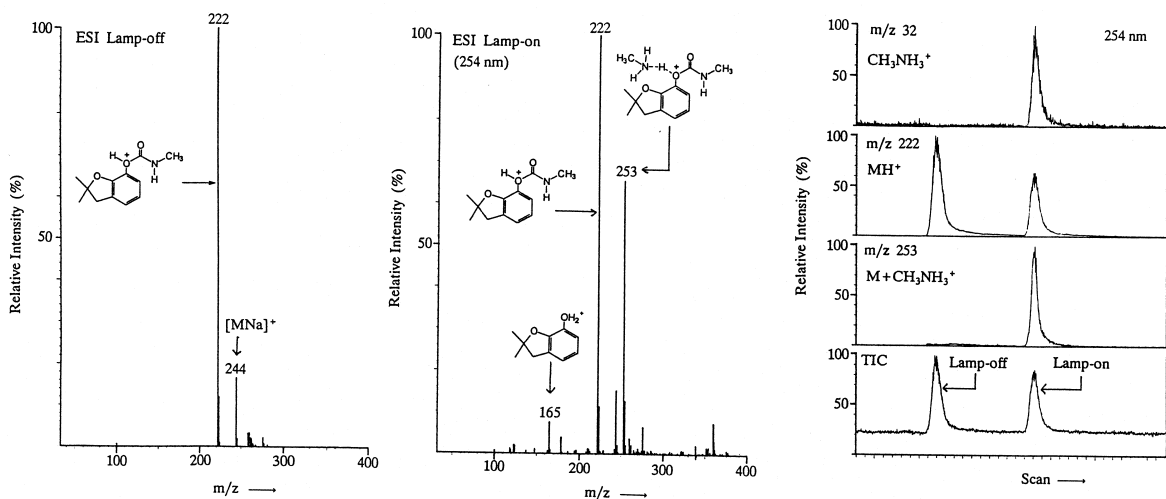


Fig. 9.  $[CH_3NH_3]^+$  and  $[M+CH_3NH_3]^+$  ions in the analysis of carbofuran. (a) ESI mass spectrum, lamp-off; (b) lamp-on; (c) LC-hv-MS ion traces under lamp-off and lamp-on conditions (full-scan flow injection analysis, ca. 5 ng/injection;  $\lambda=254$  nm, 10 m photoreactor).

**References**

- [1] J.R. Plimmer, *Residue Rev.* 33 (1971) 47.
- [2] D.G. Crosby and M.-Y. Li, in P.C. Kearny and D.D. Kaufman (Editors), *Degradation of Herbicides*, Marcel Dekker, New York, 1969.
- [3] P.C. Kearney, C.S. Helling, *Residue Rev.* 25 (1969) 25.
- [4] B.D. Cavell, *Pestic. Sci.* 10 (1979) 177.
- [5] D.A. Volmer, K. Levsen, *J. Am. Soc. Mass Spectrom.* 5 (1994) 655.
- [6] D.A. Volmer, J.G. Wilkes, K. Levsen, *Rapid Commun. Mass Spectrom.* 9 (1995) 767.
- [7] S. Sennert, D.A. Volmer, K. Levsen, G. Wünsch, *Fresenius J. Anal. Chem.* 351 (1995) 642.
- [8] D.A. Volmer, D.L. Vollmer, J.G. Wilkes, *LC·GC* 14 (1996) 216.
- [9] R.D. Voyksner and K. Keever, in H.-J. Stan (Editor), *Analysis of Pesticides in Ground and Surface Water*, Springer, Berlin, 1995.
- [10] J. Slobodnik, A.C. Hogenboom, J.J. Vreuls, J.A. Rontree, B.L.M. van Baar, W.M.A. Niessen, U.A.Th. Brinkman, *J. Chromatogr.* 741 (1996) 59.
- [11] S. Lacorte, D. Barceló, *J. Chromatogr.* 712 (1995) 103.
- [12] S. Chiron, J. Abian, M. Ferrer, F. Sanchez-Baeza, A. Messeguer, D. Barceló, *Environ. Toxicol. Chem.* 14 (1995) 1287.
- [13] S. Chiron, E. Martinez, D. Barceló, *J. Chromatogr.* 665 (1994) 283.
- [14] J. Abian, G. Durand, D. Barceló, *J. Agric. Food Chem.* 41 (1993) 1264.
- [15] I.S. Krull and W.R. LaCourse, in I.S. Krull (Editor), *Reaction Detection in Liquid Chromatography*, Marcel Dekker, New York, 1986.
- [16] R.G. Luchtefeld, *J. Chromatogr. Sci.* 23 (1985) 516.
- [17] B.M. Patel, H.A. Moye, R. Weinberger, *J. Agric. Food Chem.* 38 (1990) 126.
- [18] C.J. Miles, H.A. Moye, *Anal. Chem.* 60 (1988) 220.
- [19] R.E. Straub, R.D. Voyksner, *J. Am. Soc. Mass Spectrom.* 4 (1993) 578.
- [20] K.P. Bateman, S.J. Locke, D.A. Volmer, *J. Mass Spectrom.* 32 (1997) 297.
- [21] D.A. Volmer, J.O. Lay, S.M. Billedeau, D.L. Vollmer, *Anal. Chem.* 68 (1996) 546.
- [22] D.A. Volmer, J.O. Lay, S.M. Billedeau, D.L. Vollmer, *Rapid Commun. Mass Spectrom.* 10 (1996) 715.
- [23] I.S. Lurie, D.A. Cooper, I.S. Krull, *J. Chromatogr.* 629 (1993) 143.
- [24] M.A. Luke, H.T. Masumoto, T. Cairns, H.K. Hundley, *J. Assoc. Off. Anal. Chem.* 71 (1988) 415.
- [25] M.A. Luke, J.E. Froberg, H.T. Masumoto, *J. Assoc. Off. Anal. Chem.* 58 (1975) 1020.
- [26] W. Schwack, G. Kopf, *Z. Lebensm. Unters. Forsch.* 197 (1993) 264.
- [27] P. Cabras, M. Melis, F. Cabitza, M. Cubeddu, L. Spanedda, *J. Agric. Food Chem.* 43 (1995) 2279.
- [28] E. Romero, P. Schmitt, M. Mansour, *Pestic. Sci.* 41 (1994) 21.
- [29] G.J. Harkness, C.H.J. Wells, *Pestic. Sci.* 12 (1981) 215.
- [30] D. Sen, C.H.J. Wells, *Pestic. Sci.* 12 (1981) 339.
- [31] S.R. Dixon, C.H.J. Wells, *Pestic. Sci.* 14 (1983) 448.
- [32] S.R. Dixon, C.H.J. Wells, *Pestic. Sci.* 21 (1987) 155.
- [33] S.R. Dixon, C.H.J. Wells, *Pestic. Sci.* 25 (1989) 255.
- [34] P. Cabras, L. Spanedda, C. Tuberosa, M. Gennari, *J. Chromatogr.* 478 (1989) 250.
- [35] S.K. Nag, P. Dureja, *J. Agric. Food Chem.* 45 (1997) 294.
- [36] W.M. Horspool, *Aspects of Organic Photochemistry*, Academic Press, London, 1976, p. 238.
- [37] C. Olmedo, L. Deban, E. Barrado, Y. Castrillejo, L. Herrero, *Electrochim. Acta* 14 (1994) 2237.
- [38] J.P.M. Vink, S.E. van der Zee, *Pestic. Sci.* 46 (1996) 113.
- [39] N.R. Parekh, A. Walker, S.J. Roberts, S.J. Welch, *J. Appl. Bacter.* 77 (1994) 467.
- [40] P. Schmitt, D. Freitag, Y. Sanlaville, J. Lintemann, A. Kettrup, *J. Chromatogr. A* 709 (1995) 215.
- [41] D.W. Kolphin, S.J. Kalkhoff, *Environ. Sci. Technol.* 27 (1993) 134.
- [42] P.H. Mazzocchi, M.P. Rao, *J. Agric. Food Chem.* 20 (1972) 1957.
- [43] P. Raha, A.K. Das, *Chemosphere* 21 (1990) 99.
- [44] P.K. Freeman, K.D. McCarthy, *J. Agric. Food Chem.* 32 (1984) 873.
- [45] P.K. Freeman, E.M.N. Ndiip, *J. Agric. Food Chem.* 32 (1984) 877.
- [46] A. de Kok, M. Hiemstra, U.A.Th. Brinkman, *J. Chromatogr.* 623 (1992) 265.
- [47] D.A. Volmer, K. Levsen, M. Hönig, D. Barcelo, J. Abian, B.L.M. van Baar, U.A.Th. Brinkman, *J. Am. Soc. Mass Spectrom.* 6 (1995) 656.
- [48] R.J. Vreeken, W.D. van Dongen, R.T. Ghijssen, U.A.Th. Brinkman, *Int. J. Environ. Anal. Chem.* 54 (1994) 119.